

The Impact of Hydrodynamic Mixing on Supernova Progenitors

Patrick A. Young^{1,2}, Casey Meakin², David Arnett², & Chris L. Fryer^{1,3}

payoung@lanl.gov, cmeakin@as.arizona.edu, darnett@as.arizona.edu,
fryer@lanl.gov

ABSTRACT

Recent multidimensional hydrodynamic simulations have demonstrated the importance of hydrodynamic motions in the convective boundary and radiative regions of stars to transport of energy, momentum, and composition. The impact of these processes increases with stellar mass. Stellar models which approximate this physics have been tested on several classes of observational problems. In this paper we examine the implications of the improved treatment on supernova progenitors. The improved models predict substantially different interior structures. We present pre-supernova conditions and simple explosion calculations from stellar models with and without the improved mixing treatment at $23 M_{\odot}$. The results differ substantially.

Subject headings: stars: evolution - stars: yields - nucleosynthesis - hydrodynamics - supernovae: progenitors

1. INTRODUCTION

The predicted nucleosynthetic yields of a stellar population, as well as initial mass functions (IMFs), are dependent on stellar models. Should the underlying assumptions in a stellar evolution code change, we would expect the stellar population we infer from an observed abundance pattern or luminosity function to change as well. Conversely, predictions of the chemical evolution of galaxies will also vary.

Multidimensional hydrodynamic simulations of stellar interiors display important physical processes that are missing from formulations of stellar evolution. Bulk fluid motions

¹Theoretical Astrophysics, Los Alamos National Laboratories, Los Alamos, NM 87545

²Steward Observatory, University of Arizona, Tucson AZ 85721

³Physics Dept., University of Arizona, Tucson AZ 85721

in convective regions create an unstable boundary layer and excite internal waves which give rise to mixing and transport of energy in adjacent stably stratified layers (Press 1981; Young et al. 2005). As convective plumes enter a region of the star which is stable against oscillations (the Brünt-Väisälä frequency $N^2 > 0$) the overlying material is not engulfed by the plume and accelerated as in the convective region. Instead, the material undergoes a Lagrangian displacement and oscillates around its point of origin. The plume itself deposits its radial energy of motion into this displaced layer and spreads beneath it. The spreading of the plume and the horizontal propagation of the waves inject shear into the boundary layer. Plume impact is a stochastic process which injects energy into internal waves with a broad superposition of modes. (A detailed and excellent discussion of wave excitation can be found in Fitts, Vadas, & Øyvind (1998); Nordlund & Stein (2001); Stein & Nordlund (2001). As the fraction of pressure contributed by radiation increases, the perturbations are subjected to less restoring force. Thus the importance these processes increases with increasing stellar mass (Young et al. 2003, 2005). For supernova progenitors the effect can be dramatic.

In this paper we present simple explosion calculations for an initial mass of $23 M_{\odot}$ from models with and without the contributions from these processes, which we will call “hydro mixing” as a shorthand, implemented as in Young et al. (2005). In Section 2.1 we present interior conditions for each of the models. Section 2.2 describes hydro simulations of the O and C burning shells and their implications. Section 3 compares the explosions and discusses additional issues to be considered in a realistic supernova calculation.

2. PRE-SUPERNOVA CONDITIONS

2.1. Initial Models

We examine an initial mass of $23 M_{\odot}$ with and without hydro mixing. This mass is interesting for nucleosynthesis, being relatively numerous in the IMF while still ejecting a large amount of processed material per star into the interstellar medium (ISM) (Arnett 1996). This is also the mass of the primary member of the eclipsing binary EM Car. Apsidal motion of the binary gives us a measurement of size of the convective core on the main sequence (Young, Mamajek, Arnett, & Liebert 2001; Young et al. 2005). The hydro mixing model predicts the convective core size well, giving us one constraint on core size. We have performed 2 and 3-D simulations of the main sequence convective core and the oxygen and carbon burning shells for this mass (Meakin & Arnett 2005a,b, in prep.).

All evolution calculations were performed with the TYCHO code (Young et al. 2005). Both models use the solar composition of Grevesse & Sauval (1998). Though this abundance

pattern looks to be superseded by the (quite different) values of recent determinations (Asplund et al. 2005, and references therein), we choose to use it for comparison with earlier results. We are most interested in the comparison between the models, since a quantitatively accurate explosion requires a multidimensional calculation.

2.2. Oxygen Shell Burning Simulations

In this section we show similarities between multi-D hydro calculations and the 1D TYCHO models and discuss additional features of the stellar structure apparent only in the hydro simulations. The simulations help test the assumption of our 1D formulation as well as identifying new processes. We find the 1D treatment to be robust. These calculations extend the work of Bazàn & Arnett (1998); Asida & Arnett (2000) to higher resolution, improved initial conditions, and 3D.

The simulations used in this comparison were produced with PROMPI, a version of the PROMETHEUS PPM hydro code parallelized using domain decomposition for MPI platforms. PROMPI includes the OPAL opacities and the TYCHO equation of state and nuclear reaction subroutines with a 25 element reaction network that reproduces the energy generation of the full 177 element network to $< 1\%$. TYCHO models of $23 M_{\odot}$ with and without hydro mixing were used as initial conditions. A detailed description of both main sequence and O shell burning calculations will appear in separate papers (Meakin & Arnett 2005a,b, in prep.). Here we summarize the results from O shell models and concentrate on their consequences for pre-supernova models. Simulations were run for 2D wedges encompassing the O shell and stable regions on either side for both types of initial models (ob.2d.c and ob.2d.m). A 3D wedge (ob.3d.B) was also run for the standard initial model. Table 1 summarizes this subset of models from a larger study, with inner and outer radius, angular extent of wedge, number of zones in each dimension, and length of the simulation.

Figure 1 shows O mass fraction (top) and velocity (middle) for the 3D wedge (ob.3d.B). The yellow line on the top panel denotes the extent of the mixed region in the standard model. As soon as convection develops, the mixed region extends itself well past the original boundary and stabilizes at the new size. The same behavior of is observed in 2D (ob.2d.c) and 3D. The fluid velocities in the extended mixing region have a different character from those of the convective region below, the implications of which are discussed below. In the 2D wedge with a hydro mixing initial model (ob.2d.m), the mixed region stabilizes near the boundary predicted by the initial model. The lower panel shows ob.2d.m with the boundaries of the initial model indicated in yellow. The mixed region extends past the lower boundary of the initial model mostly because of a resolution effect. Higher resolution ameliorates the

effect, and the qualitative behavior of the boundaries is robust with changes in resolution (Meakin & Arnett 2005, in prep. Alexakis et al. 2002).

The hydrodynamic behavior observed in the simulations can be broken down into three classes. The first regime is that of full convection. Material is subject to engulfment by plumes and the flow is highly turbulent. The convective boundary and radiative regions comprise the second and third regimes, and can be roughly characterized by the Richardson number, $Ri = N^2/(\delta u/\delta r)^2$, where N is the Brünt-Väisälä frequency, and $\delta u/\delta r$ is the radial gradient of the shear velocity. Broadly speaking, Ri compares the kinetic energy in the shear to the potential energy across a stratified layer. We will refer to the region with $Ri \sim 0.25$ as the convective boundary region. Material here is not engulfed by rising plumes. Instead, plumes cause a Lagrangian displacement of material, converting the kinetic energy of the convective flow to internal wave energy. This energy conservation is ignored in 1D treatments of convection, but turns out to have a significant impact upon the structure of the star. The waves quickly become non-linear and break. This region is also subject to shear instabilities from plume spreading generating shear at the base of this region. As a result, the boundary layer becomes well mixed, and fresh fuel is entrained into the convective shell. Beyond this region the waves are linear, and we enter the third regime. Dissipation of the waves generates vorticity according to Kelvin’s Theorem and drives slow compositional mixing. These waves will also play a part in generation of large angular scale perturbations in thermodynamic and structural quantities, neutrino cooling, and intershell interactions, though we consider only the impact of compositional mixing in this paper.

The relatively close match between the 1D hydro mixing model and the dynamic O shell simulations deserves further discussion. The area inside the standard model boundary is fully convective, with a velocity pattern characteristic of convective plumes. The additional extent of mixing in ob.2d.c and ob.3d.M has a different velocity pattern. The longitudinal banding in Figure 1 is characteristic of wave motion. This is the low Ri boundary region where mixing is efficient. TYCHO evaluates a Richardson number for shear in waves and plume spreading at the driving frequency of the convection and mixes efficiently in regions with low Richardson number. As long as the spatial extent of a low Ri region produced by driving at the overall convective turnover frequency is not significantly smaller than that produced by an ensemble of plume impacts carrying the same energy, the mixing predicted in 1D should be similar to multi-D simulations. The caveat is that comparison of simulations with the hydro mixing model for O burning is limited to a single time sequence from a single set of initial conditions. More simulations are required to confirm that TYCHO predicts the extent of the boundary region correctly.

Additional features are seen in multi-D which cannot be extended to 1D, but are inter-

esting with regard to the progenitor. There is a significant wave flux in the region between the O and C burning shells with Mach numbers of several percent that gives rise to temperature and density perturbations of order 0.1-1%. Compressibility is an important feature of the flow. Since the perturbations are generated by internal waves, they have the potential to be correlated on large angular scales. As we are dealing with wedges, we cannot comment on how global these perturbations may be, save to say that the lowest order wave modes allowed by the domain are present in the simulations. Such large scale “rippling” within the progenitor may provide the seeds for asymmetries in the explosion.

3. CORE COLLAPSE MODELS AND EXPLOSIONS

Three properties of the one-D models concern us most. The density and entropy profiles of the core will determine the timing and energy of the explosion (Fryer 1999). In the neutrino-driven supernova model, neutrinos heat material just beyond the proto-neutron star core. To drive an explosion, this heated material must overcome the ram pressure of the imploding star. The success or failure of the explosion mechanism is determined, in part, by the strength of this ram-pressure which, in turn, depends upon the density in the region between ~ 1.5 - $2.0M_{\odot}$. The higher density for the progenitor including hydro mixing means that it will require more energy to explode. The explosion along with the star’s abundance profile will determine the final nucleosynthesis.

Figure 2 shows entropy (top), density (middle), and mean atomic weight (\bar{A} , bottom) versus enclosed mass for the TYCHO core collapse models and a $23 M_{\odot}$ Kepler model (Rauscher et al. 2002) with parametrized overshooting calibrated for lower mass stars (Weaver, Zimmerman & Woosley 1978). Several differences are apparent. Sharp entropy gradients are present in the mixing length and Kepler models. Entropy and species are transported by dissipative waves, and these gradients are somewhat smoothed out. Second, the density in the hydro mixing model is consistently higher. The density in the Kepler model with parametrized overshooting is an order of magnitude lower than the wave physics model outside of $2.5 M_{\odot}$, and the situation is even more extreme for the standard model. The final mass dominated by species of $A \geq 16$ is twice as large as the mixing length model. Finally, the extent of the core which has been processed by different burning stages (indicated by \bar{A}) is larger.

We calculate three explosions using an updated version of the core collapse code described in Fryer (1999). We have artificially scaled up the luminosity of the neutrinos beyond the neutrinosphere to induce an explosion. We do this by setting the free-streaming boundary for the light-bulb approximation of the Fryer (1999) code to the neutrinosphere

and artificially raising the luminosity of both the electron and anti-electron neutrinos at this boundary. This scaling is roughly 20% above a failed 1-dimensional model for our standard model and the weak wave physics model. In the strong explosion wave-physics model, we increase the neutrino luminosity by another 40%. The raised neutrino luminosities alter the structure of the collapsed core, causing the observed luminosities to not vary as much as our scaling factor, but the explosion energetics change dramatically. The energetics, remnant masses, and several interesting abundance ratios are given in Table 2. The ratio α/Fe is defined in terms of the network as

$$\frac{\sum \text{O, Ne, Mg, Si, S, Ar, Ca, Ti, Cr}}{\sum \text{Fe, Ni}} \quad (1)$$

The difference between the models is striking. For the same neutrino luminosity, the explosion energy of the hydro model drops by 65%, and the remnant mass is much larger. It requires an exceptionally powerful explosion to produce close to the same remnant mass. This energetic event would produce a very large mass of Ni. Interestingly, α/Fe is similar for the standard model and the energetic explosion of the hydro mixing model. The main difference aside from the total mass of ejected material is the C/O ratio, which is much lower in the hydro mixing model. The α/Fe for the weak explosion should be read merely as “large” since mixing during the explosion may increase the amount of Fe ejected to a few hundredths of a solar mass.

Though the mixing in late burning stages is currently unconstrained by direct observations, we may draw some general conclusions. Even if no mixing beyond the standard model were to take place after the main sequence, the apsidal motion test indicates that the core will be larger than the standard model. Overshooting models do produce larger cores, but since most schemes are empirically calibrated on lower mass stars, they are not predictive, and diverge increasingly from real stars with increasing stellar mass in the sense of underestimating core sizes. Both the hydrodynamic simulations and basic physical consistency argue for the mixing processes to continue in late burning stages, enlarging the core beyond the apsidal motion limit. We use a predictive theory for this hydrodynamic mixing in our evolution code, which is informed by multi-D simulations. Conservatively, the difference in core sizes between standard, calibrated overshooting, and hydro mixing models demonstrates the uncertainty in supernova calculations arising from progenitor models.

Though the changes in the progenitors are large, it is difficult to predict what the integrated effect on a population will be. Larger core sizes result in higher stellar luminosities, and the path of very high mass stars through the HR diagram is qualitatively very different. The IMF derived from combining models with observed luminosity functions will change. The frequency of different mass supernova progenitors and their contribution to

nucleosynthetic yields will change accordingly. A full synthetic population will be required to determine the impact of the change in progenitor models upon integrated yields.

This work was funded in part under the auspices of the U.S. Dept. of Energy, and supported by its contract W-7405-ENG-36 to Los Alamos National Laboratory, by a DOE SciDAC grant DE-FC02-01ER41176, an NNSA ASC grant, and a subcontract to the ASCI FLASH Center at the University of Chicago.

REFERENCES

- Alexakis, A., Young, Y., & Rosner, R. 2002, Phys. Rev. D, 65, 026313
- Arnett, David 1996, *Supernovae and Nucleosynthesis*, Princeton University Press
- Asida, S.M., & Arnett, D. 2000 ApJ, 545, 435
- Asplund, Martin, Grevesse, N. & Sauval, A. J. 2005, astro-ph 0410214
- Bazàn, G., & Arnett, D. 1998, ApJ, 494, 316
- Grevesse, N. & Sauval, A. J., 1998, Space Science Reviews, 85, 161
- Fitts, David C., Vadas, Sharon L., & Andreassen, Øyvind 1998, A&A, 333, 343
- Fryer, Christofer L. 1999, ApJ, 522, 413
- Nordlund, Å. & Stein, R. F. 2001, ApJ, 546, 576
- Press, W. H. 1981, ApJ, 245, 286
- Rauscher, T., Heger, A., Hoffman, R. D., & Woosley, S. E. 2002, ApJ, 576, 323
- Stein, R. F. & Nordlund, Å. 2001, ApJ, 546, 585
- Weaver, T. A., Zimmerman, G. B., & Woosley, S. E. 1978, ApJ, 225, 1021
- Young, Patrick A. & Arnett, David 2005, ApJ, 618, 908
- Young, Patrick A., Knierman, Karen A., Rigby, Jane R., & Arnett, David 2003, ApJ, 595, 1114
- Young, P. A., Mamajek, E. E., Arnett, D., & Liebert, J. 2001, ApJ, 556, 230

Table 1. Oxygen Shell Burning Models

| Model | Hydro Mixing | r_{in} cm | r_{out} cm | $\Delta\phi$ | $\Delta\theta$ | $N_r \times N_\phi \times N_\theta$ | t_{max} sec |
|---------|-----------------|----------------|-----------------|--------------|----------------|-------------------------------------|------------------|
| ob.3d.B | n | 0.3 | 1.0 | 30 | 30 | $400 \times 100 \times 100$ | 64 |
| ob.2d.c | n | 0.3 | 1.0 | 90 | ... | 400×320 | 574 |
| ob.2d.m | y | 0.3 | 1.0 | 90 | ... | 400×320 | 800 |

Table 2. Explosion Calculations

| Model | E_{expl} f.o.e. | M_{rem} M_{\odot} | M_{Ni} M_{\odot} | C/O | O/Fe | Si/Fe | Ti/Fe | α/Fe |
|--------------|----------------------|--------------------------|-------------------------|------|------|-------|------------|-------------|
| standard | 1.65 | 1.57 | 0.42 | 0.94 | 4.05 | 0.48 | 2.1^{-3} | 5.74 |
| hydro mixing | 0.57 | 6.01 | 4.0^{-4} | 0.19 | 463 | 0.60 | 2.9^{-3} | 528 |
| hydro mixing | 3.0 | 1.64 | 0.99 | 0.12 | 4.53 | 0.62 | 1.4^{-3} | 6.05 |

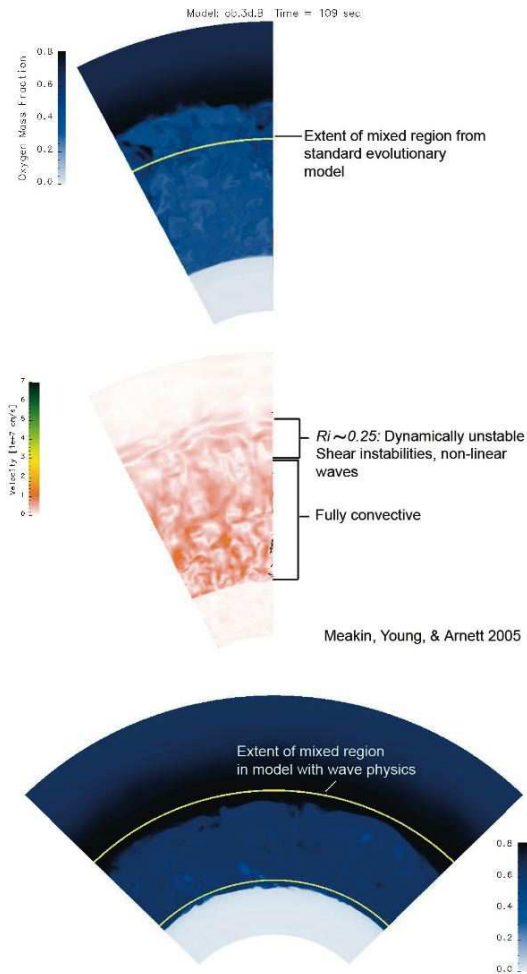


Fig. 1.— O mass fraction (top) and velocity (middle) for the 3D wedge with standard initial model (ob.3d.B) and O mass fraction for a 2D wedge with hydro mixing initial model (ob.2d.m) (bottom). The yellow line on the top panel denotes the extent of the mixed region in the 1D standard model. When convection develops, the mixed region extends itself well past the original boundary. The velocity in the extended mixing region has a different character from that of the convective region below. In the 2D wedge with hydro mixing initial model (bottom), the mixed region stabilizes near the initial model boundary (yellow). The mixed region extends past the lower boundary because of a resolution effect.

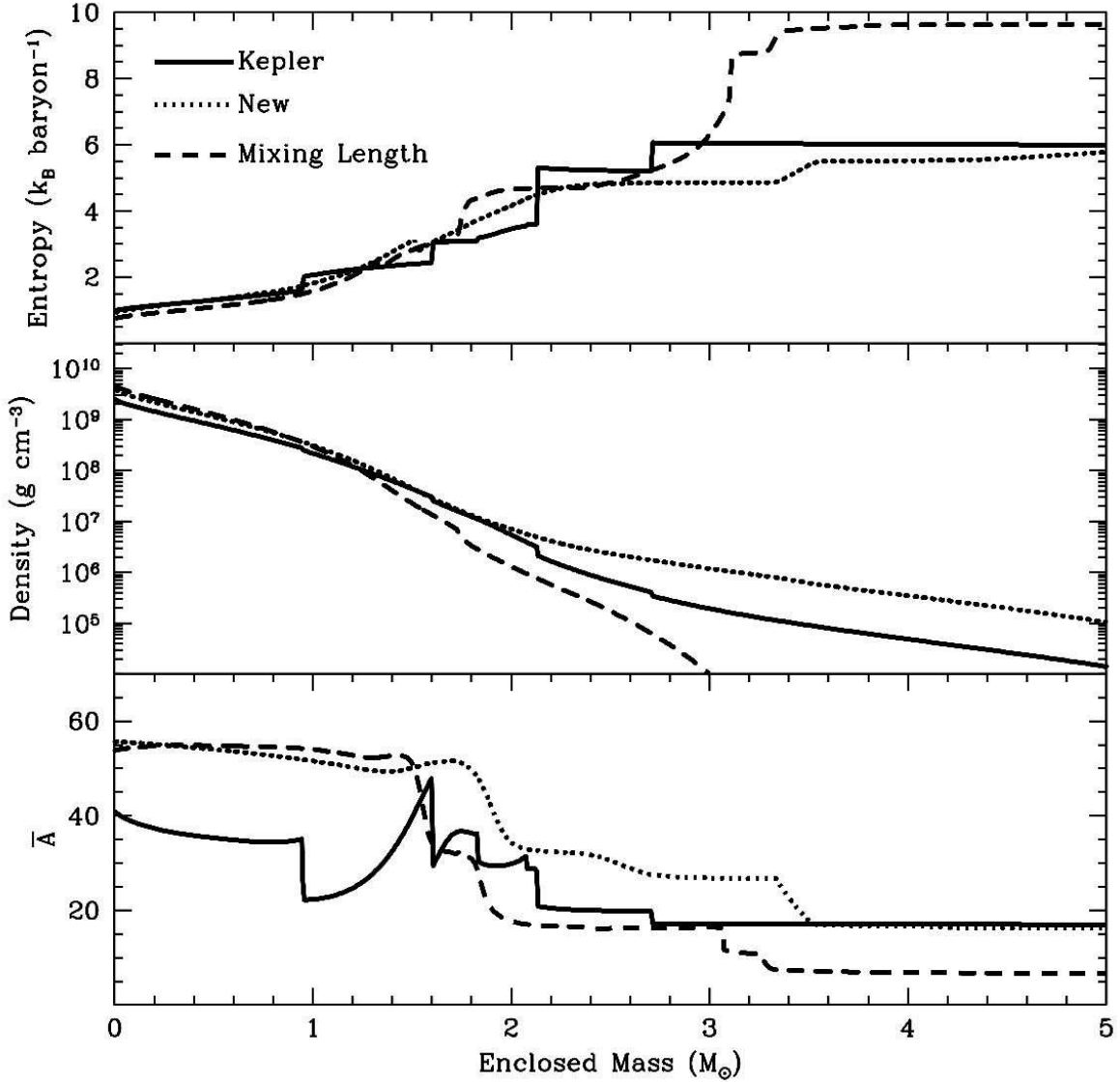


Fig. 2.— Entropy (top), density (middle), and mean atomic weight (\bar{A} , bottom) versus enclosed mass for hydro mixing (dotted), standard (dashed), and parametrized overshooting (Rauscher et al. 2002) (solid) models. The primary differences in all three plots result from the different $\bar{A} > 16$ core sizes. The entropy boundary at the outer edge of the oxygen shell moves off the plot for the hydro mixing model.